Biomaterials 32 (2011) 4293–4305

Contents lists available at ScienceDirect

Biomaterials

journal homepage: www.elsevier.com/locate/biomaterials

Angiopep-conjugated poly(ethylene glycol)-co-poly(ϵ-caprolactone) nanoparticles as dual-targeting drug delivery system for brain glioma

Hongliang Xin, Xinyi Jiang, Jijin Gu, Xianyi Sha, Liangcen Chen, Kitki Law, Yanzuo Chen, Xiao Wang, Ye Jiang, Xiaoling Fang*

Key Laboratory of Smart Drug Delivery, Ministry of Education & PLA, School of Pharmacy, Fudan University, Lane 826, Zhangheng Road, Shanghai 201203, China

ARTICLE INFO

Article history:
Received 5 January 2011
Accepted 19 February 2011
Available online 21 March 2011

Keywords:
Dual targeting
Angiopep
LRP
Blood–brain barrier
Brain glioma
PTX

ABSTRACT

Dual-targeting nanoparticle drug delivery system was developed by conjugating Angiopep with PEG–PCL nanoparticles (ANG-NP) through bifunctional PEG to overcome the limitations of low transport of chemotherapeutics across the Blood–brain barrier (BBB) and poor penetration into tumor tissue. ANG-NP can target the low-density lipoprotein receptor-related protein (LRP) which is over-expressed on the BBB and glioma cells. Compared with non-targeting nanoparticles, a significantly higher amount of rhodamine isothiocyanate-labeled dual-targeting nanoparticles were endocytosed by U87 MG cells. The anti-proliferative and cell apoptosis assay of paclitaxel-loaded ANG-NP (ANG-NP-PTX) demonstrated that ANG-NP-PTX resulted in enhanced inhibitory effects to U87 MG glioma cells. The transport ratios across the BBB model *in vitro* were significantly increased and the cell viability of U87 MG glioma cells after crossing the BBB was obviously decreased by ANG-NP-PTX. Enhanced accumulation of ANG-NP in the glioma bed and infiltrating margin of intracranial U87 MG glioma tumor-bearing *in vivo* model were observed by real time fluorescence image. In conclusion, Angiopep-conjugated PEG–PCL nanoparticles were prospective in dual-targeting drug delivery system for targeting therapy of brain glioma.

1. Introduction

Glioblastoma multiforme (GBM) is the most frequent primary central nervous system tumor, which represents the second cause of cancer death in adults less than 35 years of age [1]. Since GBM differs from other cancers by its diffuse invasion of the surrounding normal tissue, it is impossible to make the complete removal of tumor by the conventional surgical method and tumor recurrence from residual tumors is very possible [2]. Consequently, it is critical to deliver the therapeutic agent effectively to the tumor as well as to infiltrating cells that are not located in the tumor bed for GBM treatment. However, the therapeutic effects of present chemotherapy are very limited, but often causing systemic side effects, because almost all large molecule drugs and more than 98% small molecule candidate drugs are unable to reach the brain tissue due to their poor permeability across the Blood-brain Barrier (BBB) [3–5]. Another obstacle in chemotherapy is maintaining a higher concentration of therapeutic agents at the tumor site and then preventing their spread into healthy tissue [6]. To overcome the limitations of the conventional drug delivery methods, there is a need for a multifunctional carrier that can be engineered into a single nano-platform such that it can carry drugs cross the BBB and then target the tumor [7]. With this in mind, polymer nanoparticles merit attention to serve as a versatile targeting platform due to their unique structural and functional surface groups that can be used for conjugating multifunctional ligands. Nanoparticles can be designed to carry therapeutic agents that avoid interference with the immune system [8]. Furthermore, due to their small size, nanoparticles can easily flow through blood capillaries and enter the target cancer cells [9,10]. Our lab developed poly(ethylene glycol)-co-poly(ϵ-caprolactone) (PEG–PCL) nanoparticles as drug delivery system to achieve improved accumulation in the glioma tumor-bearing barin and enhanced anti-glioblastoma efficacy of model drug [11].

Receptor-mediated endocytosis is one of the mechanisms through which drug carriers cross the BBB. It is reported that various receptors are present on the luminal endothelial plasma membranes, including the transferring receptor, the insulin receptor, endothelial growth factors receptor, and low-density lipoprotein receptor [12,13]. Drug delivery systems which based on these receptors have been explored to deliver drugs across the BBB [14–16]. Low-density lipoprotein receptor-related protein (LRP), a member of the low-density lipoprotein receptor family, is highly expressed on BBB [17] and mediated the transcytosis of multiple ligands across the BBB such as lactoferrin [18], melanotransferrin

* Corresponding author. Tel.: +86 21 51980071; fax: +86 21 51980072.
E-mail address: xlfang@shmu.edu.cn (X. Fang).

0142-9612/$ – see front matter © 2011 Elsevier Ltd. All rights reserved.
doi:10.1016/j.biomaterials.2011.02.044

[19] and receptor associated protein [20]. More importantly, LRP was also over-expressed on human glioma cells [21–23]. This indicates that LRP is a potential targeted moiety for drug delivery systems, not only targeting the BBB, but also targeting the glioma.

Angiopep-2, a ligand of LRP, possesses a high brain penetration capability in both *in vitro* model of the BBB and in situ brain perfusion in mice [24,25]. It has been demonstrated that Angiopep-2 modified drug delivery system could enhance delivery gene drug [26] and near infrared fluorescent probe [27] across the BBB. However, it has not been reported that Angiopep-2 conjugation to the drug delivery system confers glioma targeting property through LRP-mediated endocytosis in the glioma cells. Based on LRP over-expression on the BBB and glioma cells, Angiopep-2 can be used not only for enhancing delivery across the BBB but also for targeting to the brain tumors. Considering the advantage of dual-targeting using the same ligand and synthetic simplicity of conjugating a single ligand, Angiopep-2 was used as a targeting moiety in the present work.

Paclitaxel (PTX), one of the most successful anticancer drugs, is the first of a new class of microtubule stabilizing agents and has demonstrable antitumor activity in glioma cell lines and animal model system of brain tumor [28,29]. However, because of the poor aqueous solubility and low therapeutic index of PTX, its clinical application is extremely limited. Furthermore, it is reported that the activity of PTX against brain tumor has been disappointing in a phase II study because of drug-resistance and poor penetration across the blood–brain barrier (BBB) [30,31].

The objective of this study was to determine the potential of Angiopep-conjugated PEG–PCL nanoparticles loaded with PTX as a dual-targeting drug delivery system in the treatment of glioma. Nanoparticles were conjugated to Angiopep for enhanced delivery across the BBB as well as for targeting the tumor via LRP-mediated endocytosis. The dual-targeting effect of PTX-loaded or fluorescently labeled nanoparticles was investigated using *in vitro* model and *in vivo* mice model.

2. Materials and methods

2.1. Materials

Methoxyl poly(ethylene glycol) (MePEG, MW 2.0 KDa), ϵ-caprolactone (ϵ-CL), RNase A, propidium iodide (PI), rhodamine B isothiocyanate (RBITC), Aprotinin, Hoechst 33342 and Stannous octoate were purchased from Sigma (St. Louis, MO, USA). Maleimidyl-poly(ethylene glycol) (Male-PEG, MW 3.5 KDa) was obtained from JenKem technology Co., Ltd (Beijing, China). Angiopep-2 (TFFYGGSRGKRNNFKTEEY) and Angiope (TFFYGGSRGKRNNFKTEEYC) were synthesized by Shanghai Gene-Pharma Co., Ltd Company (Shanghai, China). Paclitaxel was purchased from Fujian south Bio-Engineering Co. Ltd. (Fujian, China). Taxol injection (Anzatax Injection Concentrate, 30 mg/5 ml) was produced by FH Faulding & Co. Ltd. trading as David Bull Lab (Melbourne, Australia). Cremophor EL was kindly supplied by BASF Ltd. (Shanghai, China). 3-(4, 5-Dimethyl-thiazol-2-yl)-2, 5-diphenyl-tetrazolium bromide (MTT) was purchased from Sigma (St. Louis, MO, USA). Penicillin–streptomycin, DMEM, fetal bovine serum (FBS) and 0.25% (w/v) trypsin solution were purchased from Gibco BRL (Gaithersberg, MD, USA). 1, 1'-dioctadecyl-3, 3, 3', 3'-tetramethylindotricarbocyanine Iodide (Dir) was purchased from Biotium (Invitrogen, USA). Annexin V-FITC Apoptosis Detection kit and Triton X-100 were purchased from Beyotime Biotechnology Co., Ltd. (Nantong, China). All the other solvents were analytical or chromatographic grade.

2.2. Cell line

The U87 MG cell line was obtained from the Institute of Biochemistry and Cell Biology, Shanghai Institutes for Biological Sciences, Chinese Academy of Sciences (Shanghai, China). Brain capillary endothelial cells (BCECs) were kindly provided by Prof. X. G. Jiang (School of pharmacy, Fudan University).The both kinds of cells were cultured in DMEM medium, supplemented with 10% FBS, 1% nonessential amino acids, 100 IU/ml penicillin and 100 μg/ml streptomycin sulfate. All the cells were cultured in incubators maintained at 37 °C with 5% CO_2 under fully humidified conditions. All experiments were performed on cells in the logarithmic phase of growth.

2.3. Animals

Male BALB/c nude mice, aging 4–5 weeks and weighing 20 ± 2 g, were supplied by Department of Experimental Animals, Fudan University (Shanghai, China), were acclimated at 25 °C and 55% of humidity under natural light/dark conditions for 1 week before experiment. All animal experiments were carried out in accordance with guidelines evaluated and approved by the ethics committee of Fudan University (Shanghai, China).

2.4. Synthesis of dual-targeting drug delivery system

2.4.1. Synthesis of MePEG–PCL and Maleimide–PEG–PCL

The MePEG–PCL and Maleimide–PEG–PCL block copolymers were synthesized by ring-opening polymerization of ϵ-CL in dry toluene under moisture-free high purity nitrogen atmosphere, using MePEG or Maleimide–PEG as the initiator in the presence of stannous octoate as a catalyst [32]. The molecular weight of MePEG–PCL and Maleimide–PEG–PCL were determined by ^{1}H-NMR, respectively.

2.4.2. Synthesis of activated PEG–PCL nanoparticles

Activated PEG–PCL nanoparticles (NP) were prepared with a blend of MePEG–PCL and Maleimide–PEG–PCL as previously described [33]. Briefly, 22.5 mg MePEG–PCL copolymer and 2.5 mg Maleimide–PEG–PCL were dissolved in 1 ml dichlormethane (DCM). Next, 2 ml of 1% (w/v) sodium cholate solution was slowly poured into the solution and then sonicated at 200 w for 50 s (Xin zhi Biotechnology Co. Ltd., China). The resulted O/W emulsion was further diluted into 60 ml of a 0.5% aqueous sodium cholate solution and then stirred for 5 min at room temperature by a magnetic stirrer to solidify the nanoparticles. After that, the organic solvent was evaporated by rotary vacuum. The formed NP suspension was centrifuged at 12,000 rpm for 60 min at 4 °C and washed twice with deionized water. The pellets were re-suspended in 2 ml HEPES buffer (pH 7.0) and kept at 4 °C for further use.

Rhodamine isothiocyanate (RBITC) labeled nanoparticles were prepared as the same way, except that MePEG–PCL was replaced by RBITC-labeled MePEG–PCL which was synthesized as previously reported [34].

The preparation of nanoparticles loaded with PTX was the same as that of blank nanoparticles, except that about 2.5 mg of PTX was added to the copolymer solution. Dir-labeled nanoparticles were prepared by adding Dir in DCM during nanoparticle preparation.

2.4.3. Synthesis of angiopep-conjugated dual-targeting nanoparticles

For preparation of Angiopep-conjugated nanoparticles (ANG-NP), activated nanoparticles were reacted with Angiopep in HEPES buffer (pH 7.0) for 8 h under nitrogen flow at room temperature. The outer Maleimide groups of activated nanoparticles were specifically reacted with the thiol groups of Angiopep and the molar ratio of Angiopep to maleimide was 1:3 [35] The reaction mixture was then centrifuged at 12,000 rpm for 60 min at 4 °C and washed twice by PBS buffer (pH 7.4). The pellets were re-suspended in PBS (pH 7.4) and kept at 4 °C for further use. The nanoparticle concentration was determined by turbidimetry using UV2401 spectrophotometer at 600 nm (Shimadzu, Japan).

2.5. HPLC analysis

The concentration of PTX in samples was determined via HPLC on a system equipped with a LC-10ATVP pump, a SPD-10AVP UV detector (Shimadzu, Kyoto, Japan) and a HS2000 interface (Hangzhou Empire Science & Tech, Hangzhou, China). The mobile phase consisted of acetonitrile and ammonium acetate buffer solution (10 mM, pH 5.0) (50:45, v/v) was freshly prepared for each run and degassed before use. The reversed-phase column (Gemini 5 μm C18, 150 × 4.6 mm, Phenomenex, California, USA) was used at room temperature. The flow rate was set at 1.0 ml/min and the detection wavelength was 230 nm. Sample solution was injected at a volume of 20 μl. The HPLC was calibrated with standard solutions of 0.5–50 μg/ml of PTX dissolved in acetonitrile (correlation coefficient of $R^2 = 0.9995$). The limit of quantification was 0.5 ng/ml. The coefficients of variation (CV) were all within 3.5%.

2.6. Characterization of angiopep-conjugated dual-targeting nanoparticles

The morphology of the ANG-NP was studied by transmission electron microscopy (Joel JEM-1230, Japan) after negative staining with phosphotungstic acid solution (2%, w/v).

The particle size distribution and Zeta Potential were measured by the light scattering method using a Nicomp Zeta Potential/Particle Size (model 380XLS, NicompTM, Santa Barbara, CA, USA). The analyses were performed with 5 mW He-Ne laser (632.8 nm) at a scattering angle of 90°at 25 °C.

2.7. Drug-loading coefficient, encapsulation ratio and in vitro release

The drug loading coefficient (DL%) and encapsulation ratio (ER%) of PTX-loaded PEG–PCL nanoparticles (NP-PTX) and PTX-loaded PEG–PCL nanoparticles modified with Angiopep (ANG-NP-PTX) were investigated as previously described [11].

The *in vitro* release behavior of PTX from ANG-NP-PTX was monitored in an aqueous medium containing 1 M sodium salicylate by dialysis method [36,37].1 ml of PTX-loaded nanoparticle solution (containing 0.1 mg PTX) was introduced into a dialysis bag (MWCO = 14000 Da, Greenbird Inc., m containing 1 M sodium salicylate by dialysis method [36,37]. Shanghai, China) and the end sealed dialysis bag was submerged fully into 50 ml of 1 M sodium salicylate solution at 37 °C with stirring at 100 rpm for 96 h. At appropriate time intervals, 0.2 ml aliquots were withdrawn and replaced with an equal volume of fresh medium. The concentration of PTX in samples was determined by HPLC as described above with correction for the volume replacement.

The *in vitro* release kinetics of Dir was also investigated by dialysis method. Briefly, Dir-loaded nanoparticles solution after being removed free Dir via CL-4B column (Hanhong Chemical Co. LTD, China) was introduced into a dialysis bag (MWCO = 14000 Da, Greenbird Inc., Shanghai, China) and submerged fully into PBS (pH 7.4) solution at 37 °C with stirring at 100 rpm for 48 h. At appropriate time intervals, 0.4 ml aliquots were withdrawn and replaced with an equal volume of fresh medium. The concentration of Dir in samples was determined by fluoro-spectrophotometer (F-1000, Hitachi, Tokyo, Japan).

2.8. U87 MG glioma cellular uptake and competition assay

U87 MG cells were seeded at a density of 5×10^4 cells/well in 24-well plates (Corning Coaster, Tokyo, Japan) and incubated for 24 h. Then U87 MG cells were incubated with RBITC-labeled ANG-NP and NP at the concentration of 500 μg/ml for 30, 60 and 120 min at 37 °C. The solution was removed and the cells were washed three times with ice-cold PBS (pH 7.4) then visualized under fluorescent microscope (Leica DMI 4000B, Germany).

For the competition assay, Angiopep-2 or Aprotinin was added to the wells in advance at a concentration of 200 μg/ml. After 30 min incubation at 37 °C, the compounds were withdrawn from the wells, and 500 μg/ml RBITC-labeled ANG-NP along with Angiopep-2 or Aprotinin (each compound at a concentration of 200 μg/ml) were added and incubated for 120 min, followed by abovementioned steps. For RBITC-labeled ANG-NP at the concentration of 500 μg/ml, study was also carried out at 4 °C.

2.9. U87 MG glioma cellular uptake mechanism of ANG-NP

U87 MG cells were seeded at a density of 1×10^5 cells/well in 24-well plates and incubated for 24 h. After checking the confluency and morphology, Chlorpromazine hydrochloride (CPZ, 10 μg/mL), Sucrose (0.45 M), Filipin (5 μg/mL), Cytochalasin D (3 μM), 5–(N, N-Dimethyl) amiloride hydrochloride, (DMA, 10 μM), NaN_3 (1 mg/mL), Angiopep-2 (200 μg/mL) or Aprotinin (200 μg/mL) was added into each well and incubated for 30 min. Then the compounds were withdrawn from the wells, and RBITC-labeled ANG-NP along with different compounds (concentration of each compound was equal to that described above) was added. After 60 min incubation, the treatment solution was discarded and the cells were washed three times with ice-cold PBS. Then cells were lysed with PBS containing 1% Triton X-100 and centrifuged at 6000 g for 10 min. Fluorescence intensity of RBITC ($\lambda ex = 547$ nm, $\lambda em = 572$ nm) in supernatants were measured using a fluorescence microplate reader (Tecan Safire2, Switzerland). Fluorescence intensity was normalized with respect to total protein content. The protein content was determined using the BCA protein assay kit in accordance with the method specified by the manufacturer.

2.10. Confocal microscopy

U87 MG cells were seeded on 14-mm^2 glass coverslips that were placed in 6-well plates. After 24 h, cells were incubated with RBITC-labeled ANG-NP as described above for 60 min or 120 min at 37 °C followed by treatment with organelle-selective dyes. Cells were incubated with 10 μM Hoechst 33342 for 10 min and 75 nM Lysotracker Green for 30 min, respectively. Then, the loading solution was removed and the cell monolayers were washed three times with ice-cold PBS and examined by confocal laser scanning microscopy (Leica TCS SP2, Germany).

2.11. Antiproliferative activity against U87 MG glioma cells

U87 MG cells were seeded in 96-well plates at the density of 1×10^4 cells/well. After 24 h of culture at 37 °C with 5% CO_2, the medium was removed, and the cells were incubated for 72 h in the media containing PTX formulations, including Taxol injection, NP-PTX and ANG-NP-PTX of various concentrations. Cell survival was measured using tetrazolium salt MTT assay. Briefly, 180 μl of fresh growth medium and 20 μl of MTT (5 mg/ml) solution were added to each well. The plate was incubated for an additional 4 h, and then 200 μl DMSO was added to each well to dissolve any purple formazan crystals formed. The plates were vigorously shaken before taking measurement of relative color intensity. The absorbance at 570 nm of each well was measured by a microplate reader (Thermo Multiskan MK3, USA).

2.12. Cell apoptosis activity against U87 MG glioma cells

The cell apoptosis was first detected by assessment of nuclear morphology staining with Hoechst 33342. Briefly, U87 MG cells were seeded in 6-well plates containing a coverslip with 5×10^5 cells per well and cultured at 37 °C for 24 h. Cells were then incubated for another 24 h with Taxol, NP-PTX and ANG-NP-PTX (PTX concentration of 100 ng/ml) and culture medium as control. Samples were then fixed with 4% paraformaldehyde in PBS (pH 7.4) at room temperature for 15 min, stained for 15 min with 10 μg/ml Hoechst 33342 in PBS at room temperature and washed twice with ice-cold PBS. Cover-slips were mounted onto glass slide which were then examined under the fluorescent microscope (Leica DMI 4000B, Germany). For the quantitative analysis of apoptosis, cells were left untreated or were treated with Taxol, NP-PTX and ANG-NP-PTX (PTX concentration of 100 ng/ml) for 24 h. Then, non-adherent and adherent cells were trypsinized, centrifuged at 1000 g for 5 min, washed three times with ice-cold PBS and re-suspended in 200 μl of binding buffer. Thereafter, 5 μl of Annexin V-FITC and 10 μl of PI were added and mixed for 15 min in the dark. The stained cells were analyzed using a flow cytometer (FACSCalibur, BD, USA). Data analysis was performed using Cell-Quest software (Becton Dickinson, USA).

2.13. Transport across the BCECs monolayer and competition assay

BCECs were seeded on polycarbonate 24-well Transwell membrance of 1.0 μm mean pore size, 0.33 cm^2 surface areas (FALCON Cell Culture Insert, Becton Dickinson Labware, USA) at a density of 5×10^4 cells/well. After 4 days, the cell monolayer integrity was monitored using an epithelial voltohmmeter (Millicell-RES, Millipore, USA) to measure the transendothelial electrical resistance (TEER). Only cell monolayers with TEER above 200 Ω cm^2 were selected for experiment [26,38].

Transport ratio (%) was measured by using DMEM as a transport medium. Formulations were added into the donor chamber at a concentration of 10 μg/ml PTX, including Taxol, NP-PTX and ANG-NP-PTX, respectively. Cells then were incubated on a platform, shaking at 50 rpm at 37 °C. A volume of 600 μl sample medium was taken from the basolateral compartment at 1, 2, 4, 8 and 24 h, and replaced with an equal volume of fresh medium. The samples were freeze dried and determined by HPLC.

For the competition assay, Angiopep-2 or Aprotinin was added to the donor chamber in advanced at a concentration of 200 μg/ml. After 30 min incubation at 37 °C, the compounds withdraw from the Transwell, and ANG-NP-PTX along with Angiopep-2 or Aprotinin (concentration of each compound was equal to 200 μg/ml) was added, followed by abovementioned steps.

In another parallel experiment, ^{14}C-sucrose was added into the formulation solution to monitor the integrity of BCECs monolayers. TEER was also measured during experiment to monitor the integrity of BCECs monolayers.

2.14. Dual-targeting effects in vitro

For evaluating the dual-targeting effect of Angiopep-2 modified nanoparticles *in vitro*, the BCECs-U87 MG cells co-culture model was established. The BCECs incubated in the transwell for 4 days, and then the transwell was inserted into another 24-well culture plate where U87 MG cells had been cultured at a density of 1×10^4 cells/well for 1 day. The two kinds of cells in the transwell-chambers were co-cultured for 1 day to establish the co-cultured model *in vitro* [39]. The co-cultured model was incubated for 30 min with serum-free DMEM, Angiopep-2 (200 μg/ml) and Aprotinin (200 μg/ml), respectively. After removing the solution, different PTX formulations were applied to the apical chamber of these transwells, including Taxol, NP-PTX, ANG-NP-PTX, ANG-NP-PTX + Angiopep-2 (200 μg/ml) and ANG-NP-PTX + Aprotinin (200 μg/ml), respectively. The final concentration of PTX was 10 μg/ml. All the co-cultured cells after drug treatment were incubated for 8 h. After removal of the transwells, U87 MG further cultured for another 64 h and cell survival was then measured using MTT assay.

2.15. Dual-targeting effects in vivo

Real-time fluorescence imaging analysis was used to evaluate the dual-targeting *in vivo* of Angiopep-modified nanoparticles. U87 MG cells (5.0×10^5 cells suspended in 5 μl PBS) were implanted into the right striatum (1.8 mm lateral to the bregma and 3 mm of depth) of male Balb/c nude mice by using a stereotactic fixation device with mouse adaptor. ANG-NP and NP were labeled by Dir (Invitrogen, USA). In brief, Dir was co-dissolved with copolymer in DCM during nanoparticle preparation. Then, the free Dir was removed via CL-4B column (Hanhong Chemical Co. LTD, China). The intracranial U87 MG glioma bearing mice were injected with 100 μl of Dir-labeled ANG-NP or NP via tail vein 18 days after implantation. The mice were anesthetized with i.p. administered 10% chloral hydrate and placed on an animal plate heated to 37 °C. The fluorescent scans (from 620 nm to 900 nm) were performed at 2, 6, 12 and 24 h post i.v. using an in-vivo image system (CRi, Woburn, MA, USA).

To compare tissue and tumor distributions of ANG-NP, the mice were sacrificed at 24 h post-injection. Tumor-bearing brain and major organs, including livers, lungs, spleens, kidneys, and hearts, were dissected, washed with saline, and subjected to Maestro *In Vivo* imaging system to obtain the fluorescence images.

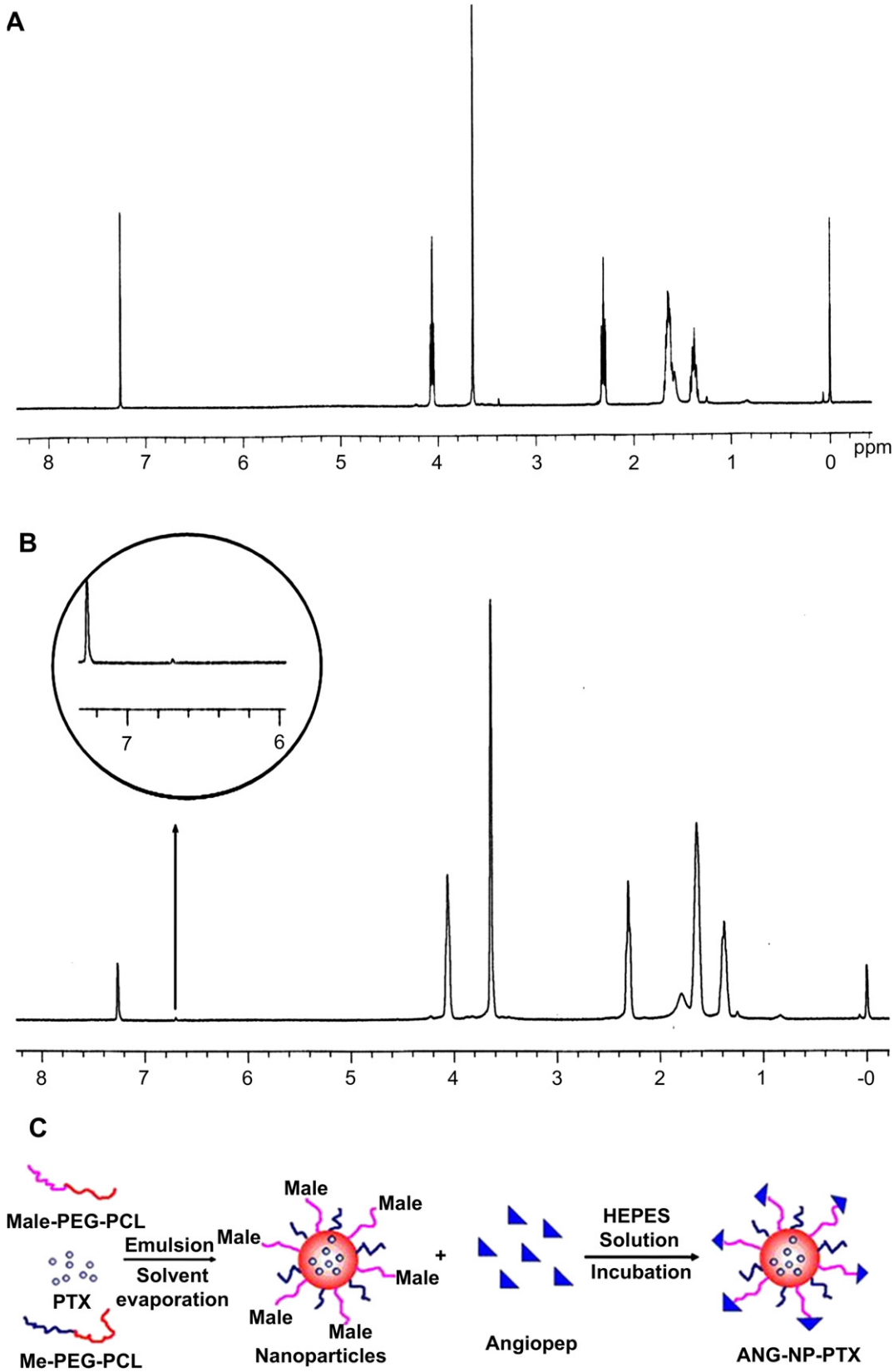

Fig. 1. ^{1}H-NMR spectrum of MePEG–PCL (A) and Maleimide–PEG–PCL(B), the strategy of constructing Angiopep-conjugated nanopaticles (C).

3. Result

3.1. Characterization of MePEG–PCL and Maleimide–PEG–PCL

In ^{1}H-NMR spectrum, the solvent peak of $CDCl_3$ was found at 7.25 ppm. There was a characteristic peak of the Maleimide group in PEG at 6.86 ppm (Fig. 1B). The peak at 3.63 ppm and 2.31 ppm were attributed to methylene units in PEG segments and ϵ-CL segments, respectively (Fig. 1A and B). From the ^{1}H integrity ratio of their methylene groups, the average molecular weight ratio of MePEG to ϵ-CL was 2000:10000 and Maleimide–PEG to ϵ–CL was 3500:10500, suggesting that the number molecular weight of MePEG–PCL and Maleimide–PEG–PCL was 12,000 and 14,000, respectively.

3.2. Characterization of the nanoparticles

PTX-loaded Angiopep-conjugated PEG–PCL nanoparticles were prepared through the outer Maleimide groups of nanoparticles specifically reacting with the thiol groups of Angiopep (Fig. 1C). The mean diameter of ANG-NP as well as NP was less than 100 nm, with an acceptably good polydispersity index (PDI $<$ 0.16). Such nanoparticles may accumulate more readily in tumor due to the Enhanced Permeability and Retention (EPR) effect [34]. The nanoparticles exhibited spherical shape of moderate uniform particle size and the particle size measured from the TEM images was in good agreement with that measured by the laser scattering technique (Fig. 2A,B).

The charge values were close to a neutral state with slight negative charges distributed around the nanoparticles (-3.08 ± 0.94 mV for NP-PTX and -3.28 ± 0.75 mV for ANG-NP-PTX).

Compared with NP-PTX, the drug loading coefficient and encapsulation ratio of ANG-NP-PTX decreased to some extent. It may due to PTX releasing from nanoparticles during the reaction between Angiopep and NP-PTX.

The *in vitro* cumulative release profiles of PTX from nanoparticles are shown in Fig. 2C. Similar to NP-PTX, ANG-NP-PTX presented biphases release behavior. After the initial burst release for about 12 h, the release rate of PTX slowed down and became an almost zero-order release. The release rate during 96 h was $77.9 \pm 2.5\%$ for NP-PTX, $78.4 \pm 1.8\%$ for ANG-NP-PTX, respectively. It is obvious that Angiopep-modified nanoparticles did not change PTX release behavior.

3.3. Uptake characteristic of nanoparticles by U87 MG cells in vitro

RBITC-labeled nanoparticles were used to investigate cellular uptake characteristic, the results of which were shown qualitatively using fluorescent images. U87 MG cells treated with either RBITC-labeled NP or RBITC-labeled ANG-NP exhibited fluorescent intensity corresponding to incubation time (Fig. 3). The cellular uptake of RBITC-labeled ANG-NP exhibited a time-dependent mode and significantly higher than RBITC-labeled NP when the incubation time ranged from 30 min to 120 min at a concentration of 500 μg/ml nanoparticles.

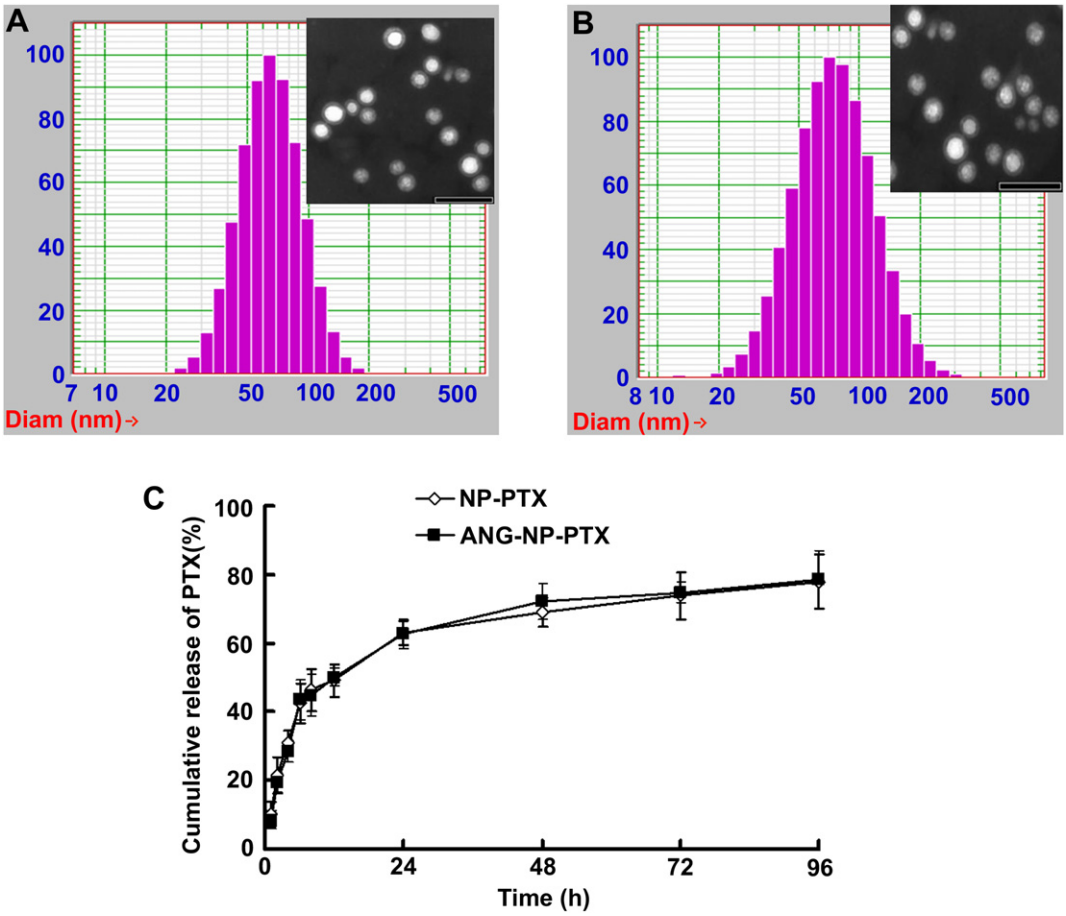

Fig. 2. Particle size distribution and TEM image of PEG–PCL nanoparticles (A) and Angiopep-modified PEG–PCL nanoparticles (B). PTX release profiles *in vitro* (C). The bar is 100 nm.

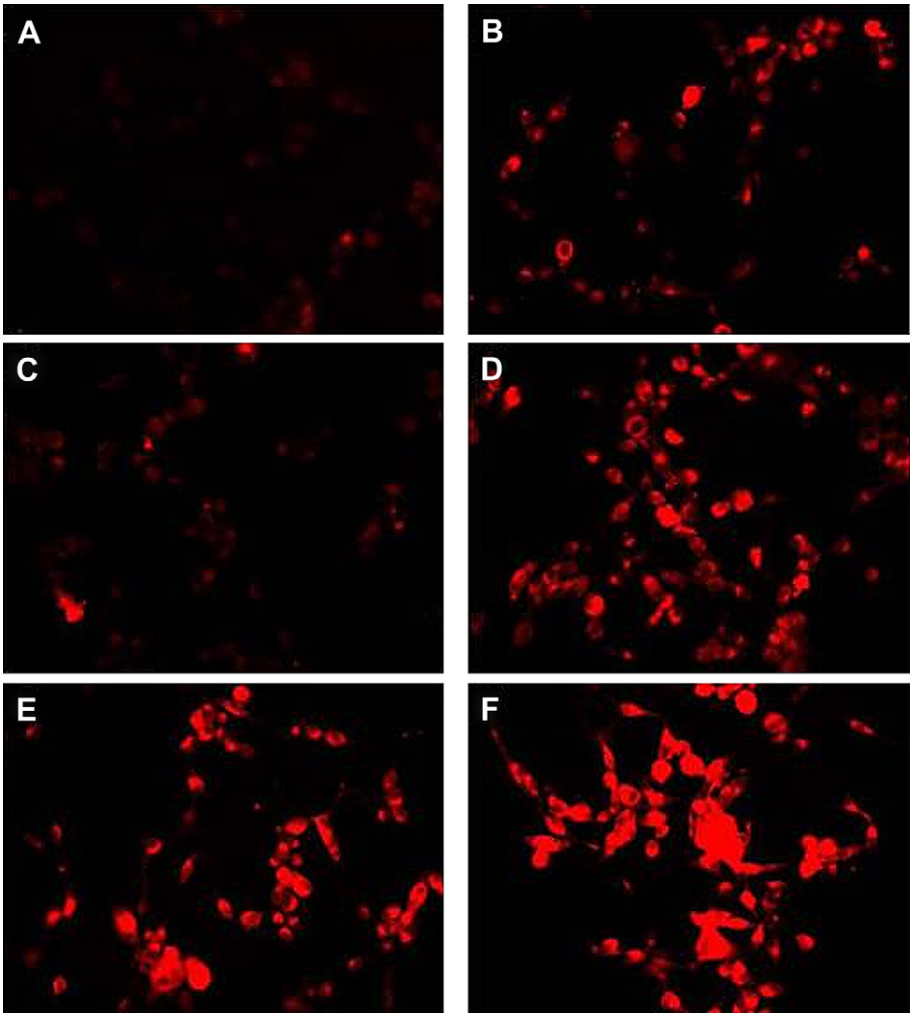

Fig. 3. Cell uptake of RBITC-labeled NP (A, C, E) and ANG-NP (B, D, F) after incubating of 30 min (*A*, B), 60 min (*C*, D) and 120 min (*E*, F) was examined by fluorescent microscopy. Concentration of nanoparticles of all samples was adjusted to 500 μg/ml. Red: RBITC. Original magnification: ×20. (For interpretation of the references to colour in this figure legend, the reader is referred to the web version of this article.)

In the competition assay, after adding different ligands of LRP, such as Angiopep-2 (Fig. 4A,C), Aprotinin (Fig. 4A,D), uptake of RBITC-labeled ANG-NP was evidently reduced. In addition, cellular uptake of RBITC-labeled ANG-NP at 4 °C was inhibited compared with that at 37 °C (Fig. 4A,B).

Therefore, the cellular uptake of ANG-NP exhibited a time-dependent and energy-dependent mode, and could be competitively inhibited by ligands of LRP.

3.4. Mechanism of cellular uptake of ANG-NP in U87 MG cells

In order to elucidate the internalization mechanism of ANG-NP, the effects of ATP depletion and endocytosis inhibitors on cellular uptake were evaluated quantitatively in U87 MG cells. Pretreatment of sodium azide (1 mg/ml) depleted cellular ATP, and decreased the cellular uptake of ANG-NP to 60.21% of the control (Fig. 5). It indicated that internalization of the ANG-NP by U87 MG cells occurred through energy-dependent endocytosis, which was consistent with above results (Fig. 4A,B).

Endocytosis, which occurs in most cells as pinocytosis, represents at least four basic mechanisms: clathrin-mediated endocytosis, caveolae-mediated endocytosis, macropinocytosis and clathrin and caveolae-independent endocytosis [40]. Filipin and Genistein were reported to inhibit caveolae-mediated endocytosis by disrupting caveolae [41–43]. Incubation with Filipin and Genistein reduced the cellular uptake of ANG-NP to 84.3% and 74.5%, respectively. It indicated the involvement of caveolae-mediated endocytosis in the cellular uptake of ANG-NP.

The effects of clathrin-mediated endocytosis on the internalization of the ANG-NP were evaluated using CPZ and sucrose, a kind of clathrin-coated pits formation-blocking agent [44–46]. Cytochalasin D and DMA, microtubule-disrupting agents [47,48], were used to evaluate the effects of macropinocytosis on the internalization of the ANG-NP. Neither of the two kinds of agents was found to influence the cellular uptake of ANG-NP ($P > 0.05$) (Fig. 5). These results suggested the minimal contribution of clathrin-mediated endocytosis and macropinocytosis on the internalization of ANG-NP by U87 MG glioma cells.

Furthermore, effect of ligands of LRP was also investigated. Ligands including Angiopep-2 and Aprotinin could significantly reduce the cellular uptake of ANG-NP by U87 MG glioma cells (Fig. 5).

3.5. Intracellular localization of ANG-NP

The intracellular localization of RBITC-labeled ANG-NP in U87 MG cells was evaluated by confocal laser scanning microscopy. Some ANG-NP were found to localize in the lysosome of U87 MG cells after 60 min incubation, showing a co-localization with the

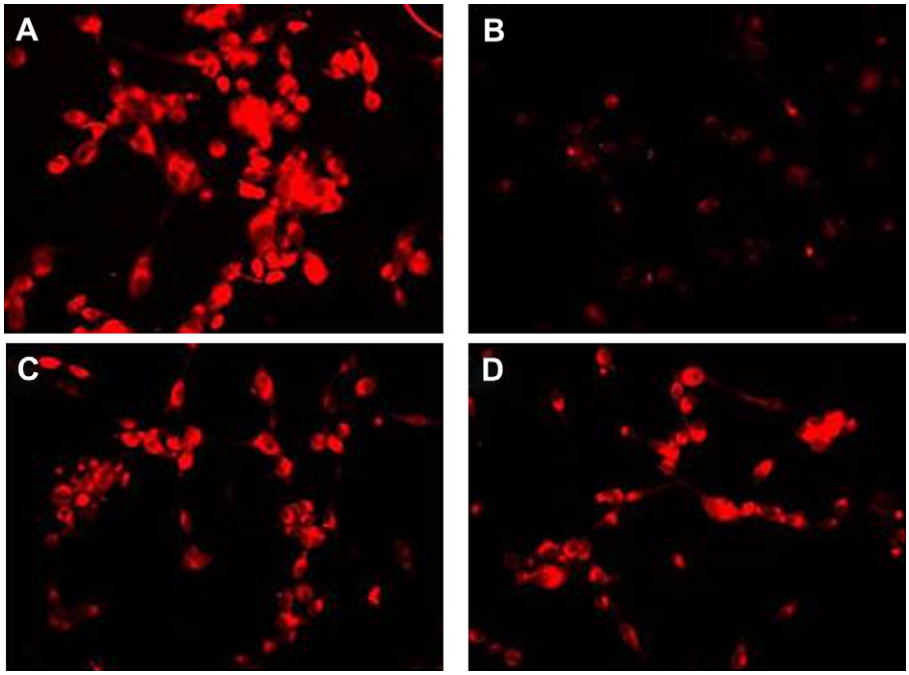

Fig. 4. Cell uptake of RBITC-labeled ANG-NP (A), ANG-NP at 4 °C (B), ANG-NP with 200 mg/ml free Angiopep-2 (C) and Aprotinin (D). Concentration of nanoparticles of all samples was adjusted to 500 μg/ml. Cell uptake was examined by fluorescent microscopy after 120 min incubation. Red: RBITC. Original magnification: ×20. (For interpretation of the references to colour in this figure legend, the reader is referred to the web version of this article.)

green fluorescence of Lyso-tracker green (Fig. 6A–D), a specific marker for lysosome. At 120 min, almost all red dots and green dots localized on the same field (Fig. 6E–H), indicating that ANG-NP taken up by the cells were delivered to lysosomes.

3.6. Antiproliferative activity against U87 MG glioma cells

The antiproliferative effect of different PTX formulations on U87 MG cells was evaluated MTT assay (Fig. 7). The results showed that ANG-NP-PTX at various concentrations exhibited the strongest inhibitory effect to the proliferation of U87 MG cells among various formulations.

The IC_{50} values of Taxol and ANG-NP-PTX toward U87 MG cells were 0.225 ± 0.024 μg/ml and 0.066 ± 0.008 μg/ml, respectively. The IC_{50} value of PTX nanoparticles modified with Angiopep was 3.4 times lower than that of Taxol. Comparisons between the drug-loaded nanoparticles showed that the IC_{50} value of ANG-NP-PTX was 3.8 folds lower than that of NP-PTX (0.248 ± 0.017 μg/ml), indicating that the antiproliferative effect of the drug-loaded nanoparticles was markedly elevated by modifying with Angiopep.

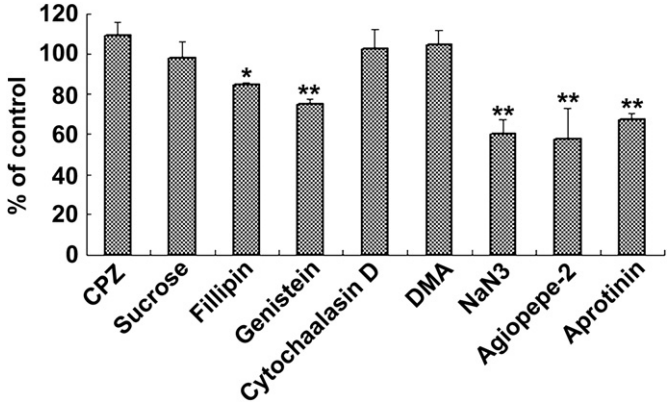

Fig. 5. Effects of inhibitors on cellular uptake of RBITC-labeled ANG-NP in U87 MG cells. Fluorescence intensity of RBITC in untreated cells, representing the maximum internalized amount of RBITC-labeled ANG-NP, was taken as control. *$p<0.05$, **$p<0.01$, compared with Control ($n = 3$).

3.7. Cell apoptosis of U87 MG glioma cells

To examine whether the encapsulation of PTX in Angiopep-conjugated nanoparticles modifies cell apoptosis, the Hoechst 33342 staining method was used to provide evidence for PTX-induced apoptotic cell death. The nuclei of untreated U87 MG glioma cells showed homogenous fluorescence with no evidence of segmentation and fragmentation after Hoechst 33342 staining (Fig. 8A). In contrast, the cell nuclei became severely fragmented when the cells were treated with PTX formulations for 24 h (Fig. 8C,E,G), suggesting the nuclei were segmentated into dense nuclear parts and further distributed into apoptotic bodies.

For quantitative analysis, Annexin V-FITC Apoptosis Detection kit was used to stain the cells and the percentage of cell apoptosis was determined by flow cytometer (Fig. 8B,D,F,H). The percentage of early and late apoptosis of Taxol-treated U87 MG glioma cells was 5.46 ± 1.28% and 18.27 ± 2.24%, respectively, while ANG-NP-PTX caused 10.28 ± 2.09% and 23.6 ± 0.14% of early and late cell apoptosis. In comparisons between the drug-loaded nanoparticles, the percentage of early and late apoptosis of ANG-NP-PTX treated U87 MG glioma cells was evidently higher than that of NP-PTX (5.55 ± 1.53% and 16.04 ± 1.34%). This was consistent with *in vitro* cytotoxicity, indicating that ANG-NP-PTX induced more early and late apoptosis, due to higher uptake of PTX via LRP receptor-mediated endocytosis, and produced higher cytotoxicity than NP-PTX.

3.8. Transport across the BCECs monolayer and competition assay

The transport ratios across the BCECs monolayer *in vitro* over a period of 24 h are shown in Fig. 9A. The transport ratio was

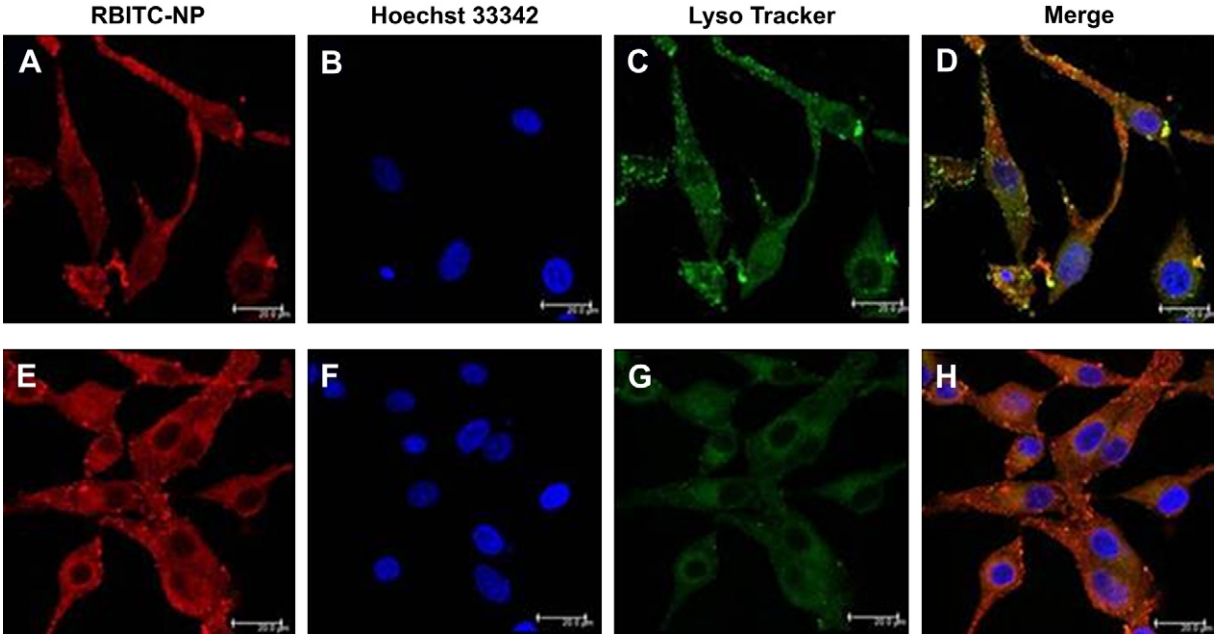

Fig. 6. Cellular location of ANG-NP, photos were taken after cells incubated with ANG-NP for 60 min (A–D) or 120 min (E–H). Red: RBITC-labeled ANG-NP (A, E). Blue: Hoechst 33342 (B, F). Green: Lysotracker Green (C, G). Yellow: Lysotracker Green co-localized with RBITC-labeled ANG-NP (D, H). Bar: 20 μm. (For interpretation of the references to colour in this figure legend, the reader is referred to the web version of this article.)

4.57 ± 0.85% for Taxol, 7.67 ± 1.30% for NP-PTX and 13.29 ± 1.09% for ANG-NP-PTX, respectively. The results indicated that the transport of PTX across the BCECs monolayer was significantly increased when PTX nanoparticles were coupled with Angiopep.

In the competition assay (Fig. 9B), Angiopep-2 or Aprotinin, was added in advance. The transport ratio of ANG-NP-PTX was significantly decreased ($P < 0.01$) due to free Angiopep-2 or Aprotinin competitively binding with LRP on BCECs, demonstrating that the transport of ANG-NP-PTX across the BBB could be significantly increased through LRP receptor-mediated endocytosis.

The integrity of the BCECs monolayer *in vitro* was monitored by TEER and permeability of ^{14}C-sucrose during experiment. TEER value of BCECs monolayer remained higher than 200 Ω cm^2 and the permeability of ^{14}C-sucrose was not significantly different from that of control.

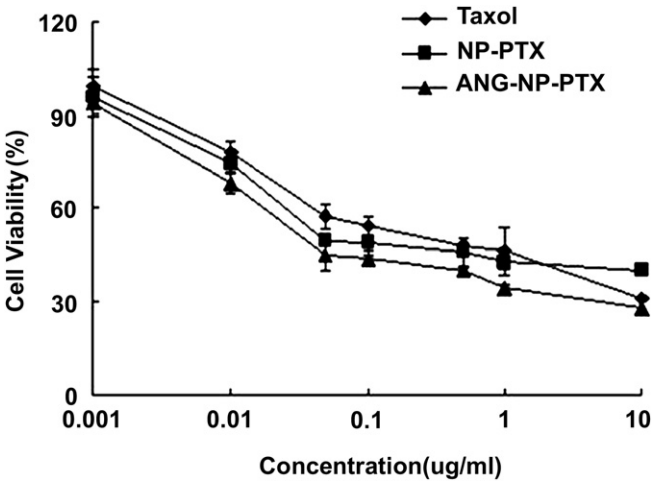

Fig. 7. In vitro cytotoxicity of various formulations of PTX against U87 MG cells ($n = 3$).

3.9. Dual-targeting effects in vitro

In order to analyze the potential dual-targeting effect of ANG-NP-PTX in mimicking the Blood-Brain-Tumor-Barrier (BBTB) *in vivo*, a BCECs-U87 MG glioma cells co-culture model was established and used for evaluation. The cell viability (%) of U87 MG cells for ANG-NP-PTX after crossing the BCECs monolayer was less than that of NP-PTX and Taxol ($p < 0.01$)(Fig. 10). The cell inhibitory effect of ANG-NP-PTX was significantly reduced by addition Angiopep-2 or Aprotinin to incubation solution ($p < 0.01$) (Fig. 10). It demonstrated that PTX-loaded nanoparticles modified with Angiopep exhibited a significant potency of transporting across the BBB and targeting the U87 MG cells, which called "dual-targeting effect".

3.10. Dual-targeting effects in vivo

The *in vivo* potential dual-targeting effect of ANG-NP was determined non-invasively in intracranial U87 MG glioma tumor-bearing nude mice, based on the fluorescence of Dir-labeled nanoparticles. After given through the tail vein, time-dependent biodistribution was observed using non-invasive NIRF imaging in live animals. Compared with NP group, the fluorescence signal in the tumor-bearing brain of ANG-NP group was much stronger at any time post-injection ranged from 2 h to 24 h (Fig. 11A).

Ex vivo evaluation of excised tissues (heart, liver, spleen, lung, and kidney) and tumor-bearing brain at 24 h post-injection showed an obvious tumor-bearing brain accumulation of the nanoparticles (Fig. 11B). The fluorescence located on the tumor position of brain for NP group, indicating that PEG–PCL nanoparticles could accumulate in glioma tissue via the EPR effect. However, the fluorescence distributed all over the brain including glioma bed and infiltrating margin for ANG-NP group, suggesting that PEG–PCL nanoparticles modified with Angiopep not only accumulated in glioma bed via EPR effect but also transported across the BBB and then targeted glioma infiltrating margin via LRP receptor-mediated endocytosis on the BBB and glioma cells. Hence, ANG-NP exhibit

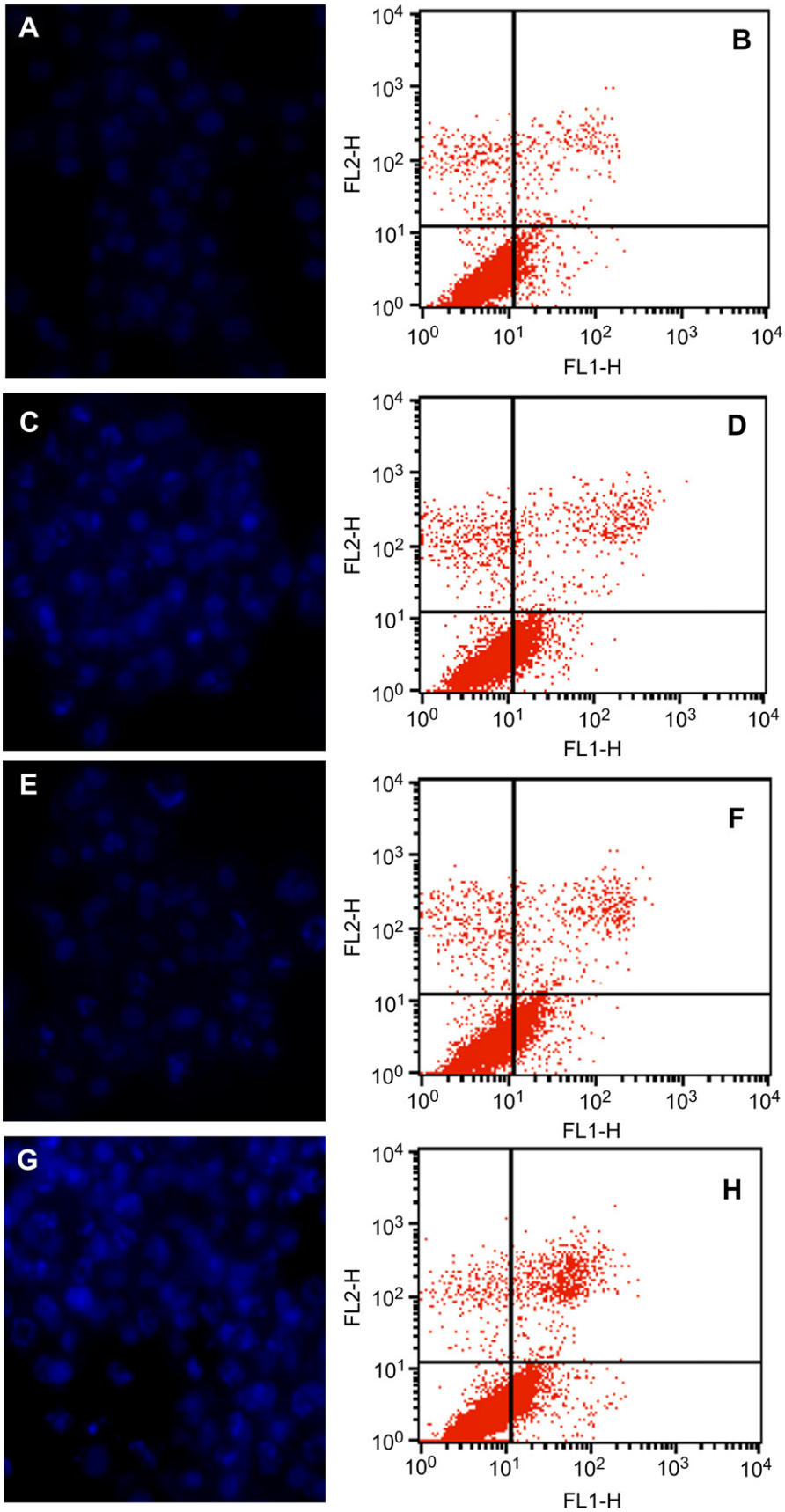

Fig. 8. Induction of apoptosis on U87 MG glioma cells by Taxol (C, D), NP-PTX (E, F) and ANG-NP-PTX (G, H) after incubation for 24 h at equivalent PTX concentration (100 ng/ml). Normal U87 MG glioma cells without any treatment served as the control (A, B). Fluorescence micrographs of U87 MG glioma cell nuclei labeled by Hoechst 33342 (A, C, E and H). Flow cytometry used staining of Annexin V-FITC and PI (B, D, F and H). Original magnification: ×20.

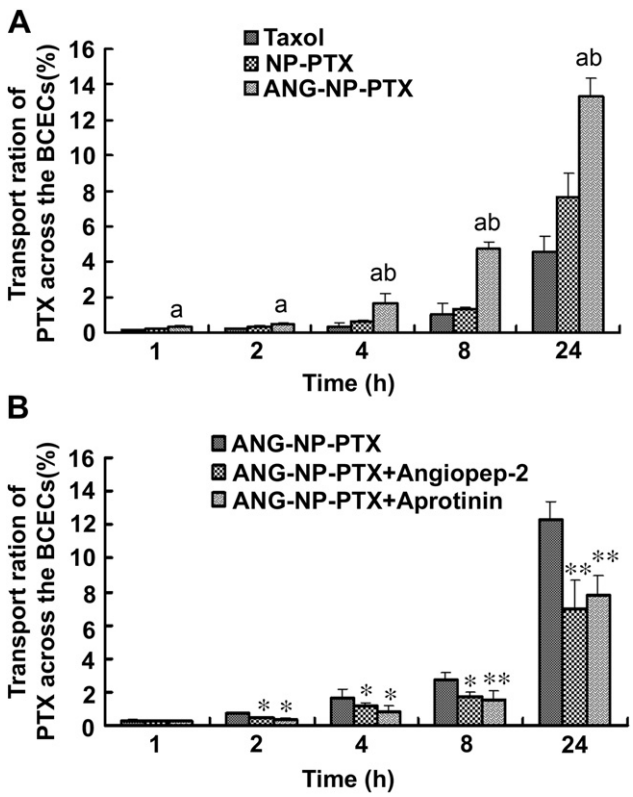

Fig. 9. The transport ratios (%) across the BCECs monolayer *in vitro* of ANG-NP-PTX during 24 h(A); The transport ratio (%) across the BCECs monolayer *in vitro* with the competition assay that the BCECs monolayer was preconditioned Angiopep-2 or Aprotinin for 30 min, and followed by applying ANG-NP-PTX at designated time points, respectively(B). Data are present as the mean + SD. a, $p<0.05$, compared with Taxol; b, $p<0.05$, compared with NP-PTX; *$p<0.05$, **$p<0.01$, compared with ANG-NP-PTX.

potential dual-targeting effect *in vivo* in intracranial U87 MG glioma tumor-bearing model. However, accumulation of the injected nanoparticles in the reticuloendothelial system (RES) was detected in either group treated with NP or ANG-NP.

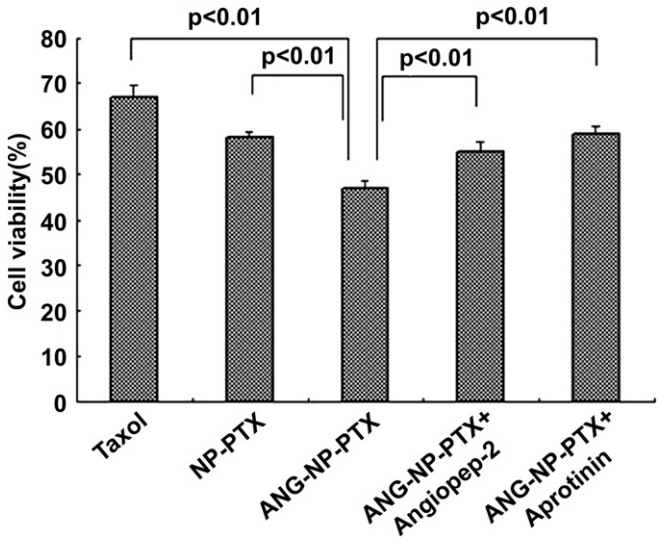

Fig. 10. The dual-targeting effect: cell viability of Taxol, NP-PTX, ANG-NP-PTX, ANG-NP-PTX+Angiopep-2, ANG-NP-PTX+Aprotinin against U87 MG cells after crossing the BBB *in vitro* ($n = 3$).

4. Discussion

In spite of decades of research, the quality of life and prognosis of GMB patients are very disappointing since it is too difficult to treat due to the aggressive growth and islets of cells remaining after surgical excision of the glioma, which lead to recurrence of the tumor. Conventional drug delivery methods cannot deliver adequate amounts of chemotherapeutic agents into brain to kill glioma cells because of the existence of BBB and tumor barrier. In recent years, the emphasis for treatment of glioma has been the identification of receptors targets on the BBB and glioma cells for the delivery of drug into brain and tumor. Such receptors target could maximize chemotherapeutic agents into brain and tumor and minimize the systemic toxic effects [7].

Among these receptors, LRP is not only over-expressed on BBB [49] but up-regulated on human glioma cells such as U87 MG and SF-539 [18]. It has been demonstrated that LRP could bind numerous ligands including lipoproteins, protease/protease inhibitor complexes and lipoprotein lipase-enriched lipoproteins [50] and mediate transport of ligands across endothelial cells of the BBB [17]. Among the ligands of LRP, Angiopep-2, a novel peptide of 19 amino acids derived from the Kunitz domain, possesses a higher *in vitro* and *in vivo* LRP-mediated brain penetration capability than other proteins, such as transferrin and aprotinin [24,25]. An Angiopep-2/PTX conjugate, named ANG1005, could improve delivery of PTX to brain and entered the clinical phase I in 2007 to treat patients with advanced solid tumors and brain metastases tumors [28,51]. In the present study, we developed a novel dual-targeting nanoparticles system by conjugating with Angiopep-2, which transported drug across the BBB and then targeted brain glioma. The Angiopep-conjugated PEG–PCL nanoparticles exhibited enhanced uptake of U87 MG glioma cells *in vitro* and accumulation in tumor-bearing brain *in vivo*. The Angiopep-conjugated PTX-loaded PEG–PCL nanoparticles exhibited stronger inhibition and apoptosis toward U87 MG glioma cells in monolayer model and co-culture model.

Similar to ANG1005, ANG-NP-PTX system was also designed to deliver PTX into brain via LRP-mediated endocytosis. More importantly, ANG-NP-PTX system offers a number of advantages over ANG1005. First, Solutol HS15/Ringer's HEPES (25/75, v/v), a non-ionic surfactant, was used as a solubilizer for ANG1005. The safety of the injected solubilizer is not very clear. It is known that 50: 50 (v/v) mixture of Cremophor EL (polyoxyl 35 castor oil) and dehydrated alcohol, a solubilizer for Taxol, is associated with serious side effects, such as hypersensitivity, nephrotoxicity and neurotoxicity as well as effects on endothelial and vascular muscles, causing vasodilatation, labored breathing, lethargy and hypotension [52], and may interfere with taxane pharmacokinetics and antitumor activity [53]. ANG-NP-PTX system greatly improved the solubility of PTX and avoided organic solvent. Second, the surfaces of ANG-NP-PTX system were modified by hydrophilic PEG chains which extended the circulation time of PTX in the blood system. Third, in terms of selective delivery, ANG-NP-PTX nanoparticles have a potential inherent advantage over ANG1005 as free drug molecules can diffuse into normal brain as well as tumor tissue but nanoparticles have a more selective delivery via the EPR effect within solid tumors [54].

In the ANG-NP-PTX system, PCL was chosen as drug carrier as it is a biodegradable polymer approved for human use by U.S. FDA and widely used in drug delivery applications [55]. Angiopep, which was synthesized by adding a cysteine to the N-termial of Angiopep-2 [26], was linked to nanoparticles by bifunctional PEG. In order to maximize the exposure of maleimide groups of nanoparticles to facilitate conjugation with Angiopep, the chain of Maleimide–PEG (MW, 3500) was longer than that of MePEG (MW, 2000) (Fig. 1)

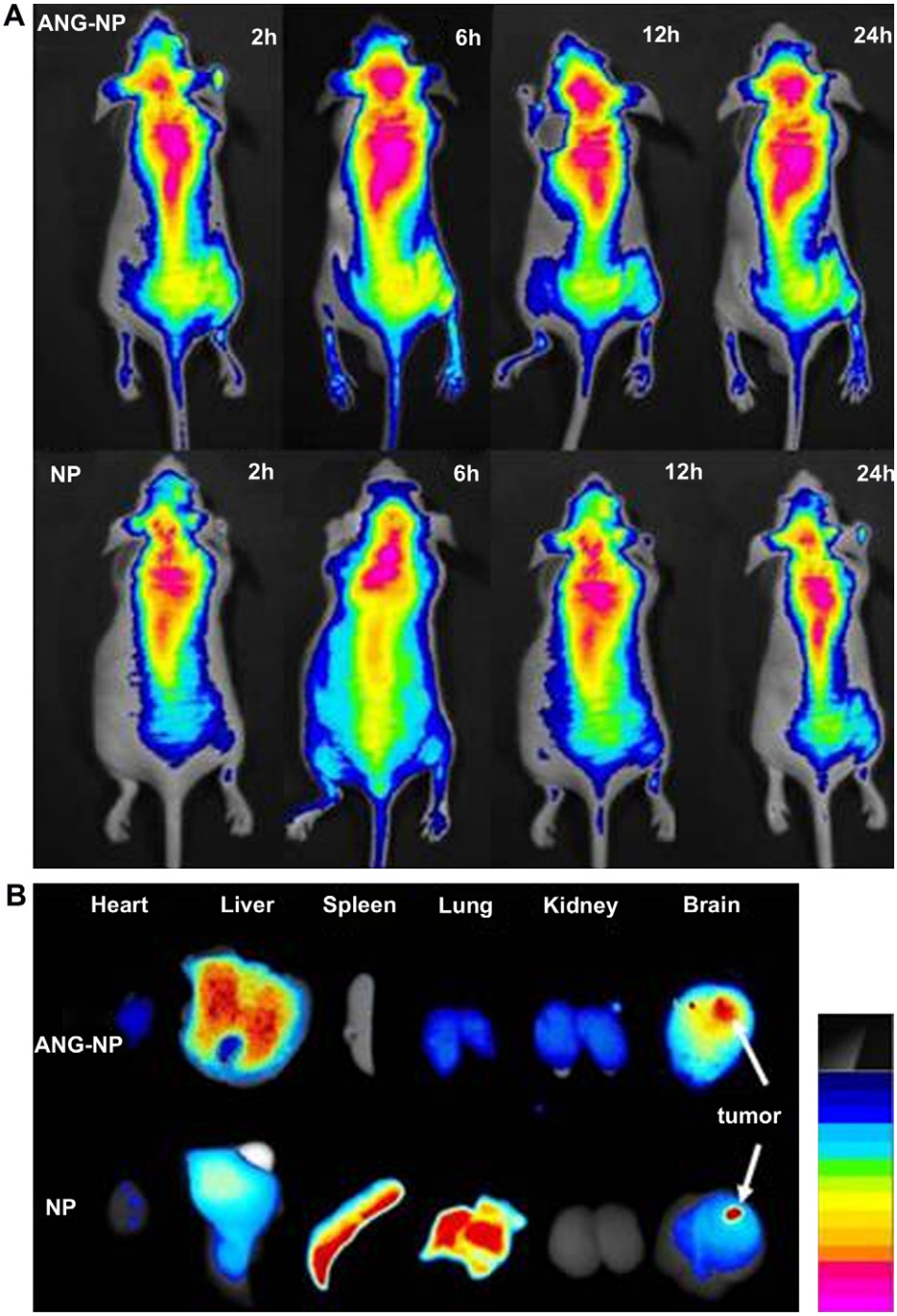

Fig. 11. *In vivo* fluorescence imaging of intracranial U87 MG glioma tumor-bearing nude mice after intravenous injection of nanoparticles (A). Images of dissected organs of mice bearing intracranial U87 MG glioma sacrificed 24 h after intravenous injection of nanoparticles (B). *Arrow*: the position of tumor.

After conjugated with Angiopep, the particle size was a little bigger than activated nanoparticles (Fig. 2A, B). But they are still less than 100 nm, which is optional for improving the pharmacokinetics of nanoparticles [56] and advantageous for endocytosis by brain capillary endothelial cells [57].

The cellular uptake of PEG–PCL nanoparticles in U87 MG cells was enhanced by conjugating Angiopep (Fig. 3). The internalization of ANG-NP was time-dependent (Fig. 3) and energy-dependent (Fig. 4A,B). Precondition with Angiopep-2 (Fig. 4A,C) or Aprotinin (Fig. 4A,D), ligands of LRP, the cellular uptake of ANG-NP was significantly reduced as LRP were competitively binding with free ligands. The same competitive inhibition effects occurred in the BCECs monolayer model and BCECs-U87 MG cells co-culture model of ANG-NP-PTX, because LRP is also over-expressed on BCECs.

As for the nanoparticle internalization mechanisms of Angiopep-conjugated PEG–PCL nanoparticles system, the main mechanism was caveolae-mediated endocytosis while the minimal contribution of clathrin-mediated endocytosis and macropinocytosis involved on the internalization by U87 MG cells (Fig. 5). It was reported that Angiopep-modified PAMAM–PEG/DNA nanoparticles were internalized by BCECs through clathrin- and caveolae-mediated endocytosis, and also partly through macropinocytosis [26]. This is not

paradoxical because charge, shape, material composition, surface chemistry of nanoparticles and cell type are important parameters that determine cellular entry of nanoparticles through definitive endocytic route [58]. Results of cellular localization (Fig. 6) showed that ANG-NP taken up by the cells were delivered to lysosomes, in which a great percentage of the drug is trapped in the organelle or degraded. Fortunately, PTX, a microtubule-stabilizer, would impair lysosomal integrity [59], which might increase the rate of escape of ANG-NP-PTX from the lysosome.

The MTT and cell apoptosis assay demonstrated that PTX formulations resulted in obvious inhibitory effects to U87 MG cells, suggesting that glioma cells were sensitive to PTX. The results from the cytotoxicity curves and flow cytometry of cell apoptosis indicated that NP-PTX was comparable effectiveness of Taxol (Figs. 7 and 8). After modifications of PTX-loaded nanoparticles with Angiopep, the IC_{50} value was decreased and the percentage of early and late apoptosis of U87 MG cells was increased, demonstrating that the endocytosis by the U87 MG cells was increased by ligand modification. This could be explained by that the increased endocytosis is mediated by the specific binding between Angiopep and LRP followed by increased internalization of U87 MG cells.

To imitate the dual barrier (BBB and tumor barrier) of glioma *in vivo*, a BCECs-U87 MG glioma cells co-culture model was established to evaluate the dual-targeting effects of ANG-NP-PTX *in vitro* [60–62]. From the results of the transport ratios across the BCECs monolayer model *in vitro* (Fig. 9), it was calculated that the concentration of PTX in basolateral compartment could reach median lethal dose (LD_{50}) against U87 MG cells after 8 h transport from the donor chamber. As a result, the transwell containing PTX formulations were incubated for 8 h and then removed in the co-culture model assay. The inhibitory effects on U87 MG cells were significantly enhanced by PTX-loaded nanoparticles modified with Angiopep(Fig. 10), which strongly confirmed the anti-proliferation effect, cell apoptosis of U87 MG cells and the transport across the BCECs monolayer model *in vitro*. It indicated that ANG-NP-PTX exhibited strong dual-targeting effects *in vitro*.

To further verify the dual-targeting effects of ANG-NP *in vivo*, intracranial U87 MG glioma tumor-bearing nude mice were used to investigate the distribution of Dir-labeled nanoparticles. The *in vitro* release kinetics of Dir-loaded nanoaprticles was investigated by dialysis method and the results exhibited that less than 1% of Dir released from the nanoaprticles within 48 h. Therefore, the Dir combining with nanoparticles together penetrated into brain and tumor but not free Dir in the imaging analysis [27,63,64]. The results from *in vivo* and *ex vivo* imaging photos of tumor-bearing brain indicated that Angiopep-modification enhanced nanoparticle accumulation in the glioma bed and infiltrating margin. It suggested that ANG-NP exhibited strong dual-targeting effects: Angiopep mediated the transport of the ANG-NP across BBB through LRP as grade I targeting, followed by endocytosis of ANG-NP via recognition of LRP on the surfaces of U87 MG as grade II targeting. The accumulation of the nanoparticles in the liver could be interpreted as classical passive targeting of the nanoparticles. By presenting PEG on the surfaces of nanopartilces, the rate of RES uptake of the nanoparticles can be greatly reduced, allowing the nanoparticles to have an increased chance to distribute to the target tissue. However, the majority of the injected nanoparticles are still uptake by RES, typically leaving 2–10% nanoparticles being distributed to the target tissue [56].

5. Conclusion

Angiopep-conjugated PEG–PCL nanoparticles constructed in this study were proved to increase the transport of the nanoparticles across the BBB and afterwards target the brain glioma by *in vitro* co-culture model and *in vivo* imaging of brain fluorescence. Angiopep-conjugated PEG–PCL nanoparticles were internalized by U87 MG glioma cells through caveolae-mediated endocytosis and displayed higher cell uptake and stronger inhibition and apoptosis toward glioma cells due to LRP-mediated endocytosis. We have demonstrated here that Angiopep-conjugated PEG–PCL nanoparticles are prospective dual-targeting drug delivery system for therapy of brain glioma.

Acknowledgements

We are grateful for the financial supports from the National Basic Research Program of China 973 program (2007CB935802); National Natural Science Foundation of China (30873177) and National Science and Technology Major Project (2009ZX09310-006).

References

[1] Allard E, Passirani C, Benoit JP. Convection-enhanced delivery of nanoparticles for the treatment for brain tumors. Biomaterials 2009;30:2302–18.
[2] Ong BY, Ranganath SH, Lee LY. Paclitaxel delivery from PLGA foams for controlled release in post-surgical chemotherapy against glioblastoma multiforme. Biomaterials 2009;30:3189–96.
[3] Pardridge WM. BBB-Genomics: creating new openings for brain-drug targeting. Drug Discov Today 2001;6:381–3.
[4] Pardridge WM. Crossing the blood-brain barrier: are we getting it right? Drug Discov Today 2001;6(1):1–2.
[5] Pardridge WM. The lack of BBB research. Drug Discov Today 2002;7(4):223–6.
[6] Minchinton AI, Tannock IF. Drug penetration in solid tumors. Nat Rev Cancer 2006;6:583–92.
[7] Dhanikula RS, Argaw A, Bouchard JF, Hildgen P. Methotrexate loaded polyether-copolyester dendrimers for the treatment of gliomas: enhanced efficacy and intratumoral transport capability. Mol Pharm 2008;5(1):105–16.
[8] McCarthy JR, Weissleder R. Multifunctional magnetic nanoparticles for targeted imaging and therapy. Adv Drug Deliv Rev 2008;60(11):1241–51.
[9] Koo YE, Reddy GR, Bhojani M, Schneider R, Philbert MA, Rehemtulla A, et al. Brain cancer diagnosis and therapy with nanoplatforms. Adv Drug Deliv Rev 2006;58(14):1556–77.
[10] Moghimi SM, Hunter AC, Murray JC. Nanomedicine: current status and future prospects. FASEB J 2005;19(3):311–30.
[11] Xin HL, Chen LC, Gu JJ, Ren XQ, Zhang W, Luo JQ, et al. Enhanced anti-glioblastoma efficacy by PTX-loaded PEGylated poly (ϵ-caprolactone) nanoparticles: in vitro and in vivo evaluation. Int J Pharm 2010;402:238–47.
[12] Smith MW, Gumbleton M. Endocytosis at the blood-brain barrier: from basic understanding to drug delivery strategies. J Drug Target 2006;14:191–214.
[13] Visser CC, Voorwinden LH, Crommelin DJ, Danhof M, de Boer AG. Characterization and modulation of the transferrin receptor on brain capillary endothelial cells. Pharm Res 2004;21(5):761–9.
[14] Gabathuler R, Arthur G, Kennard M, Chen Q, Tsai S, Yang J, et al. Development of a potential protein vector (NeuroTrans) to deliver drugs across to the blood-brain barrier. Int Congr Ser 2005;1277:171–84.
[15] Muruganandam A, Tanha J, Narang S, Stanimirovic D. Selection of phage-displayed llama single-domain antibodies that transmigrate across human blood-brain barrier endothelium. FASEB J 2002;16(2):240–2.
[16] Pang ZQ, Feng L, Hua RQ, Chen J, Gao HL, Pan SQ, et al. Lactoferrin-conjugated biodegradable polymersome holding doxorubicin and tetrandrine for chemotherapy of glioma rats. Mol Pharm 2010;7(6):1995–2005.
[17] Bell RD, Sagare AP, Friedman AE, Bedi GS, Holtzman DM, Deane R, et al. Transport pathways for clearance of human Alzheimer's amyloid beta-peptide and apolipoproteins E and J in the mouse central nervous system. J Cereb Blood Flow Metab 2007;27:909–18.
[18] Fillebeen C, Descamps L, Dehouck MP. Receptor-mediated transcytosis of lactoferrin through the blood-brain barrier. J Biol Chem 1999;274(11):7011–7.
[19] Demeule M, Poirier J, Jodoin J, Bertrand Y, Desrosiers RR, Dagenais C, et al. High transcytosis of melanotransferrin (p97) across the blood-brain barrier. J Neurochem 2002;83:924–33.
[20] Pan W, Kastin AJ, Zankel TC, van Kerkhof P, Terasaki T, Bu G, et al. Efficient transfer of receptor-associated protein (RAP) across the blood-brain barrier. J Cell Sci 2004;117:5071–8.
[21] Maletinska L, Blakely EA, Bjornstad KA. Human glioblastoma cell lines: levels of low-density lipoprotein receptor and low density lipoprotein receptor-related protein. Cancer Res 2000;60:2300–3.
[22] Yamamoto M, Ikeda K, Oshshima K, Tsugo H, Kimura H, Tomonaga M, et al. Increased expression of low density lipoprotein receptor-related protein/α2-macroglobulin receptor in human malignant astrocytomas. Cancer Res 1997;57:2799–805.
[23] Bu G, Maksymovitch EA, Geuze H, Schwartz AL. Subcellular localization and endocytic function of low density lipoprotein receptor-related protein in human glioblastoma cells. J Biol Chem 1994;269:29874–82.
[24] Demeule M, Régina A, Ché C, Poirier J, Nguyen T, Gabathuler R, et al. Identification and design of peptides as a new drug delivery system for the brain. J Pharmacol Exp Ther 2008;324(3):1064–72.

[25] Demeule M, Currie JC, Bertrand Y, Ché C, Nguyen T, Régina A, et al. Involvement of the low-density lipoprotein receptor-related protein in the transcytosis of the brain delivery vector angiopep-2. J Neurochem 2008;106(4):1534–44.
[26] Ke WL, Shao K, Huang RQ, Han L, Liu Y, Li JF, et al. Gene delivery targeted to brain using an Angiopep-conjugated polyethyleneglycol-modified polyamidoamine dendrimer. Biomaterials 2009;30(36):6976–85.
[27] Shen J, Zhan CY, Xie C, Meng QG, Gu B, Li C, et al. Poly(ethylene glycol)-block-poly(d, l-lactide acid) micelles anchored with angiopep-2 for brain-targeting delivery. J Drug Target 2010;6:1–8.
[28] Régina A, Demeule M, Ché C, Lavallée I, Poirier J, Gabathuler R, et al. Antitumor activity of ANG1005, a conjugate between paclitaxel and the new brain delivery vector Angiopep-2. Br J Pharmacol 2008;155:185–97.
[29] Desai A, Vyas T, Amiji M. Cytotoxicity and apoptosis enhancement in brain tumor cells upon coadministration of paclitaxel and ceramide in nanoemulsion formulations. J Pharm Sci 2008;97:2745–56.
[30] Chang SM, Kuhn JG, Robins HI, Schold SC, Spence AM, Berger MS, et al. A Phase II study of paclitaxel in patients with recurrent malignant glioma using different doses depending upon the concomitant use of anticonvulsants: a north American brain tumor consortium report. Cancer 2001;91:417–22.
[31] Postma TJ, Heimans JJ, Luykx SA, van Groeningen CJ, Beenen LF, Hoekstra OS, et al. A phase II study of paclitaxel in chemonaive patients with recurrent high-grade. Ann Oncol 2000;11:409–13.
[32] Pang ZQ, Lu W, Gao HL, Hu KL, Chen J, Zhang CL, et al. Preparation and brain delivery property of biodegradable polymersomes conjugated with OX26. J Control Release 2008;128:120–7.
[33] Meng F, Engbers GHM, Feijen J. Biodegradable polymersomes as a basis for artificial cells: encapsulation, release and targeting. J Control Release 2005;101:187–98.
[34] Zhu ZS, Li Y, Li XL, Li RT, Jia ZJ, Liu BR, et al. Paclitaxel-loaded poly(N-vinylpyrrolidone)-b-poly(ϵ-caprolactone) nanoparticles: preparation and antitumor activity in vivo. J Control Release 2010;142:438–46.
[35] Olivier JC, Huertas R, Lee HJ, Calon F, Pardridge WM. Synthesis of pegylated immunonanoparticles. Pharm Res 2002;19:1137–43.
[36] Han LM, Guo J, Zhang LJ, Wang QS, Fang XL. Pharmacokinetics and biodistribution of polymeric micelles of paclitaxel. Acta Pharmacol Sin 2006;27:747–53.
[37] Zhang W, Hao JG, Shi Y, Li YJ, Wu J, Sha XY, et al. Paclitaxel-loaded Pluronic P123/F127 mixed polymeric micelles: formulation, optimization and in vitro characterization. Int J Pharm 2009;336:176–85.
[38] Xie Y, Ye LY, Zhang XB, Hou XP, Lou JN. Establishment of an in vitro model of Brain-blood barrier. Beijing Da Xue Xue Bao 2004;36(4):435–8.
[39] Kuhlmann CR, Lessmann V, Luhmann HJ. Fluvastatin stabilizes the blood–brain barrier in vitro by nitric oxide-dependent dephospho-rylation of myosin light chains. Neuropharmacology 2006;51:907–13.
[40] Liu J, Shapiro JI. Endocytosis and signal transduction: basic science update. Biol Res Nurs 2003;5:117–28.
[41] Chang J, Jallouli Y, Kroubi M, Yuan XB, Feng W, Kang CS, et al. Characterization of endocytosis of transferring-coated PLGA nanoparticles by the blood-brain barrier. Int J Pharm 2009;379:285–92.
[42] Aoki T, Nomura R, Fujimoto T. Tyrosine phosphorylation of caveolin-1 in the endothelium. Exp Cell Res 1999;253:629–36.
[43] Liu P, Anderson RG. Spatial organization of EGF receptor transmodulation by PDGF. Biochem Biophys Res Commun 1999;26:695–700.
[44] Roger E, Lagarce F, Garcion E, Benoit JP. Lipid nanocarriers improve paclitaxel transport through human intestinal epithelial cells by using vesicle-mediated transcytosis. J Control Release 2009;140:174–81.
[45] Tahara K, Sakai T, Yamamoto H, Takeuchi H, Hirashima N, Kawashima Y, et al. Improved cellular uptake of chitosan-modified PLGA nanospheres by A549 cells. Int J Pharm 2009;382:198–204.
[46] Abu Lila AS, Kizuki S, Doi Y, Suzuki T, Ishida T, Kiwada H, et al. Oxaliplatin encapsulated in PEG-coated cationic liposomes induces significant tumor growth suppression via a dual-targeting approach in a murine solid tumor model. J Control Release 2009;137:8–14.
[47] Xu ZH, Chen LL, Gu WW, Gao Y, Lin LP, Zhang ZW, et al. The performance of docetaxel-loaded solid lipid nanoparticles targeted to hepatocellular carcinoma. Biomaterials 2009;30:226–32.
[48] Nam HY, Kwon SM, Chung H, Lee SY, Kwon SH, Jeon H, et al. Cellular uptake mechanism and intracellular fate of hydrophobically modified glycol chitosan nanoparicles. J Control Release 2009;135:259–67.
[49] Krieger M, Herz J. Structure and functions of multiligand lipoprotein receptors: macrophage scavenger receptors and LDL receptor-related protein (LRP). Ann Rev Biochem 1994;63:601–37.
[50] May P, Herz J, Bock HH. Molecular mechanisms of lipoprotein receptor signalling. Cell Mol Life Sci 2005;62(19–20):2325–38.
[51] Thomas FC, Taskar K, Rudraraju V, Goda S, Thorsheim HR, Gaasch JA, et al. Uptake of ANG1005, a novel paclitaxel derivative, through the blood-brain barrier into brain and experimental brain metastases of breast cancer. Pharm Res 2009;26:2486–94.
[52] Weiss RB, Donehower RC, Wiernik PH. Hypersensitivity reactions from Taxol. J Clin Oncol 1990;8:1263–8.
[53] Ten tije AJ, Verweij J, Loos WJ, Sparreboom A. Pharmacological effects of formulation vehicles: implication for canner chemotherapy. Clin Pharmacokinet 2003;42:665–85.
[54] Bhojani MS, Dort MV, Rehemtulla A, Ross BD. Targeted imaging and therapy of brain cancer using theranostic nanoparticles. Mol Pharm 2010;7(6). 1921–9.
[55] Chawla JS, Amiji MM. Biodegradable poly(ϵ-caprolactone) nanoparticles for tumor targeted delivery of tamoxifen. Int J Pharm 2002;249:127–38.
[56] Li SD, Huang L. Pharmacokinetics and biodistribution of nanoparticles. Mol Pharm 2008;5(4):496–504.
[57] Huwyler J, Wu D, Pardridge WM. Brain drug delivery of small molecules using immunoliposomes. Proc Natl Acad Sci 1996;93(24):14164–9.
[58] Sahay G, Alakhova DY, Kabanov AV. Endocytosis of nanomedicines. J Control Release 2010;145:182–95.
[59] Groth-Pedersen L, Ostenfeld MS, Høyer-Hansen M, Nylandsted J, Jäättelä M. Vincristine induces dramatic lysosomal changes and sensitizes cancer cells to lysosome-destabilizing siramesine. Cancer Res 2007;67(5):2217–25.
[60] Tian W, Ying X, Du J, Guo J, Men Y, Zhang Y, et al. Enhanced efficacy of functionalized epirubicin liposomes in treating brain glioma-bearing rats. Eur J Pharm Sci 2010;41(2):232–43.
[61] Ying X, Wen H, Lu WL, Du J, Guo J, Tian W, et al. Dual-targeting daunorubicin liposomes improve the therapeutic efficacy of brain glioma in animals. J Control Release 2010;141:183–92.
[62] Du J, Lu WL, Ying X, Liu Y, Du P, Tian W, et al. Dual-targeting topotecan liposomes modified with tamoxifen and wheat germ agglutinin significantly improve drug transport across the Blood-Brain Barrier and survival of brain tumor-bearing animals. Mol Pharm 2009;6(3):905–17.
[63] Zhan CY, Gu B, Xie C, Li J, Liu Y, Liu WY, et al. Cyclic RGD conjugated poly (ethylene glycol)-co-poly(lactic acid) micelle enhances paclitaxel anti-glioblastoma effect. J Control Release 2010;143(1):136–42.
[64] Zhan CY, Yan ZQ, Xie C, Lu WY. Loop 2 of ophiophagus hannah toxin b binds with neuronal nicotinic acetylcholine receptors and enhances intracranial drug delivery. Mol Pharm 2010;7(6). 1940–7.